Current crowding issues on nanoscale planar organic transistors for spintronics applications

Tindara Verduci,[1] Guillaume Chaumy,[1] Jean-Francois Dayen,[1] Nicolas Leclerc,[2] Eloïse Devaux,[3] Marc-Antoine Stoeckel, [3] Emanuele Orgiu,[3,4] Paolo Samorì,[3] Bernard Doudin[1]

1. University of Strasbourg, CNRS, IPCMS UMR 7504, 23 rue du Loess, 67034 Strasbourg, France.

2. University of Strasbourg, CNRS, ICPEES UMR 7515, 25 rue Becquerel, 67087 Strasbourg, France.

3. University of Strasbourg, CNRS, ISIS UMR 7006, 8 allée Gaspard Monge, F-67083 Strasbourg, France.

4. Institut National de la Recherche Scientifique (INRS), EMT Center, 1650 Blvd. Lionel-Boulet, J3X 1S2 Varennes, Canada.

Abstract *The predominance of interface resistance makes current crowding ubiquitous in short channel organic electronics devices but its impact on spin transport has never been considered. We investigate electrochemically-doped nanoscale PBTTT short channel devices and observe the smallest reported values of crowding lengths, found for sub-100 nm electrodes separation. These observed values are nevertheless exceeding the spin diffusion lengths reported in the literature. We discuss here how current crowding can be taken into account in the framework of the Fert-Jaffrès model of spin current propagation in heterostructures, and predict that the anticipated resulting values of magnetoresistance can be significantly reduced. Current crowding therefore impacts spin transport applications and interpretation of the results on spin valve devices.*

Keywords: current crowding, nanodevices, organic electronics, spintronics, spin valve

1. Introduction

Current crowding in lateral devices (Fig. 1) relates to non-uniform current flowing between source and drain electrodes terminals. Contributions to the current also originate from areas of the injecting (collecting) electrodes beyond their edges, with a resulting active channel length exceeding the inter-electrode separation L_0. This issue was initially discussed for Si-based devices,[1,2] and is nowadays highly relevant for organic electronics, owing to the importance of metal/organic interfaces,[3] [4] and its predominance for short channel transistors, becoming a critical issue for nanoscale devices.

Our main motivation here is to clarify how current crowding can impact the performance of devices aimed at spin electronics applications. Organic materials have attracted significant interest for this purpose, essentially driven by the expected long spin lifetime in organics.[5] However, the low mobility of organic semiconductors severely limits the spin current propagation to a few tens of nm only,[6] eventually reaching 110 nm for C60[7] and 200 nm for PBTTT.[8] Larger values, reaching 1.1 μm, require on zero-gap single crystals at low temperatures.[9] This length scale, over which a spin current exponentially vanishes, should be compared to the length scale of current non-uniformity or 'crowding length'. This issue is particularly relevant for lateral devices relying on a staggered geometry to inject and detect a spin current. Two key questions need to be addressed: is it possible to manufacture lateral spin valve devices with organic materials exhibiting much smaller crowding length that their expected spin diffusion length? How can these current non-uniformity issues quantitatively impact the device spin-dependent performance?

Assuming ohmic injection and a semiconductor with uniform conductivity (much smaller than that of the metallic electrodes), the transmission-line approximation circuit of Fig. 1 results in the source-drain current decreasing exponentially away from the electrode edges, with a characteristic 'crowding length' L_T, given by:

$$L_T = \sqrt{\frac{r_b}{R_{Sheet}}} \qquad (1)$$

where r_b is the specific contact resistivity, i.e. the contact resistance per unit area (in $\Omega \cdot cm^2$, related to R_c in Fig. 1) and R_{Sheet} is the sheet resistance (Ω/sq, R_S in Fig. 1) of the active semiconductor layer. The circuit approximation used here applies to staggered transistor device, where a top gate added to Fig. 1 constrains current to flow at the (top) semiconductor-gate interface. It also holds for uniformly conducting layers, under the condition that one has ohmic charge injection 'perpendicular'.

Even though Eq. (1) is oversimplified for anisotropic and non-linear transport in organic materials, the model gives the essential idea of a crowding length that scales an exponential current variation away for the edges of the source and drain electrodes. It also emphasizes how the current crowding length increases when the interface resistance dominates. This becomes an increasingly important issue for device miniaturization and is particularly relevant for organic electronics devices, where the metal/semiconductor interfacial resistance is expected to largely dominate the total resistance of a device when its channel length is reduced down to the μm scale. Measurements on organic semiconductor transistors in staggered geometry indicate crowding length values typically decreasing with device channel length: $\approx 0.25L_0$ for $L_0 > 5$ μm,[10] and ≈ 600 nm for 100nm $< L_0 <$ 1μm.[11] Note that the latter results were found for several different organic semiconductor materials, with field-effect mobility values spanning the 10^{-2} - 10 cm^2/Vs range.

Spin transport in organic materials requires a spin current that can be generated, transported through an organic spacer, and detected.[5] The recent results on PBTTT rely on spin pumping from a magnetic electrode and voltage detection of the generated spin currents in a vertical geometry.[8] In order to observe this voltage signal, the spacer is required to keep the memory of the polarization of the injected spin current at best, which however exponentially decreases over a length scale defined as the intrinsic 'spin diffusion length' l_{sf} in the material. This terminology, historically defined in metallic systems where a diffusive model of transport prevails,[12] is a commonly accepted broader denomination, even though transport in organics and inorganics differ. For spin electronics applications, the archetype device is the

spin valve, made of magnetic source and drain electrodes, and relies on the change of full (charge and spin) current injection and collection when changing the relative magnetization of the electrodes between parallel and anti-parallel. This results into a significant two-terminal change of resistance with applied magnetic field (magnetoresistance, MR). Here, the current must be injected into the organic spacer, and then extracted by the collecting electrode. As the propagation of a pure spin current does not obey to the applied electric field, injection and detection in the ferromagnetic contacts can be hampered by the spin current tendency to diffuse away towards the most conductive path. This 'resistance mismatch' is expected to complicate the successful implementation of organic spin valves with significant resistance change.[13]

A vertical stack structure is the most common spin valve geometry reported in literature, but electrical shorts can mimic the reported MR attributed to spin transport through organics.[14] Planar lateral structures could alleviate such issues, with the benefit of adding gate control of the spin transport. However, successful indications of spin valve properties are scarce.[15-] Furthermore, negligible or ambiguous effects are reported when the electrode material differs from LSMO perovskite.[18-21] There is therefore a clear need for unambiguous demonstration of spin-dependent charge transfer between two ferromagnetic electrodes separated by an organic semiconductor.

As most reported lateral structures involved uniformly conducting organics and large contact electrodes, current crowding effects are expected. Furthermore, the reported spin diffusion lengths in organics (20 - 200 nm) are significantly smaller than the smallest crowding length values previously mentioned. Limiting or eliminating current crowding requires non-staggered geometries (e.g. bottom-gate bottom-contact configuration), but at the expense of efficient charge injection over a significantly thick layer of material. Severely decreasing the extension of the source-drain electrodes (along x direction in Fig. 1) is an alternative that requires dedicated lithography that can result in topographic influence on soft or suspended materials at the sub-100 nm scale. All in all, there is therefore an unavoidable need to consider the influence of current crowding on organic spintronic applications.

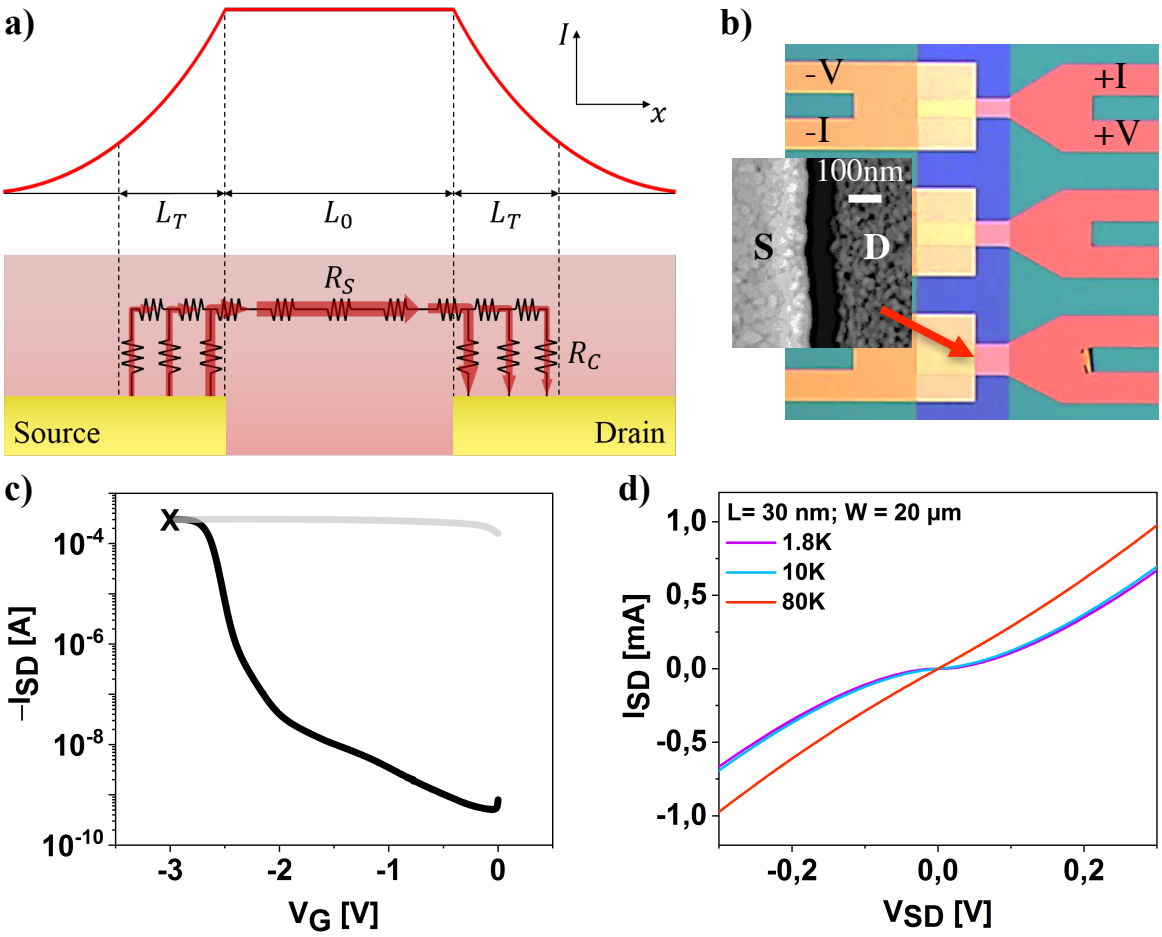

FIG. 1. a) Current crowding between two electrodes, showing the non-uniform current flowing in a resistive (R_s) thin film separated by interface resistance R_c from source and drain electrodes, with a crowding length scale L_T; b) nm-scale planar electrodes design with pseudo-four probes interconnects studied in this work (S= source, D= drain), c) transfer curve of device b) under electrolyte gating. In dark the first sweep, up to the 'X' point of saturation and maximum doping; in grey the return curve with large hysteresis, d) IV curves of device b) at low temperature, for maximum doping.

A first important outcome of current crowding is that the effective channel length is expected to be on the order of $2L_T + L_0$. Lateral device fabrication targets electrode separations ranging from 20 nm to 100 nm, reachable by standard nanolithography techniques. Previously-reported estimates of the crowding length should therefore result in an effective channel length easily one order of magnitude larger than the electrode separation, exceeding the estimates of l_{sf} in thin film organics! Models of spin transport in inorganic semiconductor devices emphasize that an effective spin injection and collection requires the channel length to be significantly smaller than l_{sf} in order to reach noticeable spin valve signals amplitudes.[22] We therefore anticipate that spin diffusion lengths exceeding the µm range might be necessary to obtain a significant spin signal for the reported designs of lateral spin valve structures.

In this paper, we want to get better and quantitative insight into the crowding lengths for sub-100 nm electrode separation length scale, and calculate how it impacts the transfer of spin information. We first provide experimental insight into the crowding length values for highly doped (C12-)PBTTT, which we consider to be among the best candidates for organic spintronics. We avoid magnetic electrodes, to alleviate the issue of their interface reactivity with the organic material.[23] In order to focus the discussion on the smallest possible effects of current crowding that one needs to consider, experiments are performed with Au electrodes, known to be ideally suited for PBTTT and therefore expected to provide minimum interface contact resistance and related crowding length values. We then calculate how current crowding,

implemented in the Fert & Jaffrès' model of spin transport,[22] quantitatively modifies the MR properties of a spin valve.

2. Experimental Results

We rely on our recently investigated 20-nm thick PBTTT films that can be highly doped using a polyelectrolyte ad-layer, as previously reported,[24,13] with mobility values reaching 10 cm^2/Vs. If we consider that the active channel has now a total length of $2L_T + L_0$ and that the area of injection/collection of charges is of the order of $W \cdot L_T$, where W is the width of the channel, a simple manipulation of Eq. (1) provides a crowding length estimate of the order of:

$$L_T \sim \frac{1}{4}\left(W\frac{R}{R_{Sheet}} - L_0\right) \qquad (2)$$

where R is the total device resistance. We summarize in Table 1 the (transmission line) crowding length values deduced from Eq. (2), for electrodes spacing in the sub-μm range (Fig. 1) and use the R_{Sheet} value for PBTTT measured on large-scale devices by the four-probes method (Fig. 1b). All results are reported for the maximum doping, at gate voltage corresponding to the onset of redox reactions at the source and drain electrodes (Figure 1d). This value ensures the best reproducibility for comparisons between very different channel lengths. See details in references [23] and [24]. Electrodes with sub-μm separation are fabricated by focused ion beam milling or angle evaporation method,[25] with resulting electrodes spaced in the 30-300 nm range (Fig. 1c). Separation values of around 80 nm are obtained by both methods, and device properties are reproduced within experimental error. Note however that good reproducibility of the large-scale conductivity values remains a bit elusive (with a factor two variability over ten or more successive experiments), owing to the intrinsic reproducibility difficulties in electrochemical doping experiments and possible non-uniformity of current flow. For Table 1, we used an average conductivity value of 440 ± 100 S/cm (with $R_{Sheet} \sim$ 1100 Ω/sq) at room temperature, decreasing by a factor 9 at 1.8K, extracted from four-probes measurements. Resistance of the device is measured at source drain voltage of 0.2 V, in the linear region for all temperatures (Figure 1e). The rather large uncertainty accounts for non-uniformity of the current and difficulties in reproducing the same conductivity over several samples. As a result, reported values in Table 1 have typical 25% uncertainty. We previously observed larger conductivity values on mm-size devices, using overnight annealing of the samples in vacuum, which possibly results in crystalline-like samples.[1324] We avoided this step, which can possibly disrupt the very small separation between Au electrodes in nanoscale devices.[25]

TABLE 1 Comparison of properties of short-channel transistors using PBTTT as the active layer under maximum electrochemical doping. The crowding length is calculated using conductivity deduced from measurements on large-scale samples (200-400 μm channel length).

L_0 [nm]/ W [μm]	T [K]	L_T [μm] ±25%	R_{CH} [Ω] ±25%	R_C [Ω] ±25%
80±10/ 30±1	300±1	**0.16**	15	6.0
	1.8±0.1	**0.06**	66	19
80/40	300	**0.48**	28	14
	1.8	**0.09**	67	23.2
80 /50	300	**0.52**	25	12
	1.8	**0.17**	85	34
30/20	300	**0.38**	43	22
	1.8	**0.20**	230	110
300/80	300	**0.50**	15	5.5
	1.8	**0.40**	79	20

Data in Table 1 present crowding length values measured at the two limit temperatures of our setup. We systematically observed a lower crowding length at the lowest temperatures. The measured crowding lengths, on the order of 100 nm at low temperature (1.8 K) and 500 nm at room temperature, are remarkably small, even though the conductivity of the organic channel is quite high. It illustrates the extremely low contact resistance of these devices, expected to be minimal when performing experiments on organic semiconductors whose bulk is electrochemically doped.

A total device resistance $R = R_{ch} + 2R_c$, is the sum of the channel resistance R_{ch} and twice the average of the source and drain contact resistance R_c. From the knowledge of L_T, and the measurement of R, estimates of $R_{ch} = R_{Sheet}\left(\frac{2L_T+L}{W}\right)$ (for electrodes extending over infinite distance in the x direction), and R_c are given in Table 1. In the limit where the crowding length is much larger than the spacing between electrodes, simple manipulations of the Eq. (1) show that:

$$2R_c \sim R_{ch} \sim \frac{1}{2}R. \qquad (3)$$

This indicates that current crowding makes charge injection occur over a larger area, up to contact resistances that balance out the whole channel resistance. Eq. (3) recalls the key criterion for efficient spin current injection and collection through a semiconducting spacer: the spin interface resistance should be of the same order as the spin channel resistance.[22] More precisely, the specific spin contact resistivity (in Ω·cm^2) defined as $r_b^* = r_b \frac{2}{1-\gamma^2}$ (where γ is the interface spin polarization of the injected current) should be in the range $r_N \frac{t_N}{l_{sf}} < r_b^* < r_N \frac{l_{sf}}{t_N}$, where the non-magnetic spacer has a spin resistance per unit area defined as $r_N = R_{sheet} \cdot t \cdot l_{sf}$ (t is the thickness of the film). As mentioned before, an active layer length much smaller than the spin diffusion length l_{sf} allows a larger window for the adequate spin interface resistance value. We recently emphasized how the large contact resistance of organic/metal interfaces is a severe bottleneck for spin current collection.[13] Crowding effects might provide opportunities to alleviate

this problem. Under the hypothesis that l_{sf}= 200 nm (largest reported length for organics) and γ = 0, values of the ratio r_b^*/r_N, between 0.1 and 6.8 results from the values of Table 1, reasonably well-centered around one. Our estimates for short-channel PBTTT devices indicate that the spin contact resistivity can indeed possibly reach the proper range of values, if the spin diffusion length is long enough.

More quantitative insight into the influence of L_T on the MR of spin valves can be gained through numerical simulations of the MR values by using Fert and Jaffrès' expressions for the difference ΔR between antiparallel and parallel resistance values (their Eq. 24)[22] and the parallel resistance R^P (their Eq. 26))[22], with the *MR* defined as their ratio. The thickness of the non-magnetic layer (t_N in their notation) is replaced here by the length *L,* separating points of injection and collection of the current lines, yielding therefore $MR(L) \equiv {\Delta R(L)}/{R^P(L)}$. One can also define the magnetoconductance as $MG(L) \equiv {[R^P(L) - R^{AP}(L)]}/{R^{AP}(L)}$, in order to ensure $MR(L) = MG(L)$. To introduce current crowing effect, we suppose that the total current flowing in the gap between two electrodes separated by L_0 is the sum of currents injected-detected from larger distances *L*, with current magnitude varying exponentially over a scale L_T (Fig. 1):

$$i(L) = i_0 e^{-\frac{L-L_0}{2L_T}}. \qquad (3)$$

We can then approximate the magnetoconductance of the total current i_0 as the weighted sum of the magnetoconductance of partial currents $i(L)$ building it. More specifically, when writing it in the more usual form of magnetoresistance ratio:

$$MR_{L_T}(L_0) = \frac{1}{2L_T}\int_{L_0}^{\infty} MR(L) e^{-\frac{L-L_0}{2L_T}}\, dL \qquad (4)$$

where the prefactor $\frac{1}{2L_T}$ normalizes the integral of the exponential function. Fig. 2 illustrates how non-zero L_T values modify the MR. The normalized lengths $\tilde{L}_0, \tilde{L}, \tilde{L}_T,$ corresponds to L_0, L, L_T divided by the spin diffusion length value, as ${t_N}/{l_{sf}}$ enters into the MR equations. Calculations are performed using the optimum value of r_B^* that maximizes MR, with resulting asymptotic maximum MR ratio of 33% (defined by the choices of β = 0.43 and γ = 0.5). The semi-log plot illustrates that, for $L \gg l_{sf}$, the MR decreases exponentially over a l_{sf} scale: $MR(L) \propto e^{-L/l_{sf}}$, as expected. From inspection of Fig. 2, several main consequences of introducing the crowding length can be pointed out:

1) the MR ratio is reduced by approximately one order of magnitude when the crowding length reaches $4l_{sf}$ (Fig. 2a)

2) $MR_{L_T}(L_0) \approx MR_0(L_0 + \Delta)$, which indicates that considering crowding effects results in the MR of electrodes separated by a larger effective length, increased by an amount Δ. The inset of Fig. 2b shows that $\Delta \sim \sqrt{l_{sf} L_T}$, where this geometrical mean value differs from the hypothesis of an effective channel length increased by $2L_T$. Qualitatively, the results is that the *MR* varies exponentially with the distance, which by itself has an exponentially decreasing contribution to the current

3) the value of the spin diffusion length deduced from a series of data with increasing distance between electrodes, is not significantly affected by current crowding.

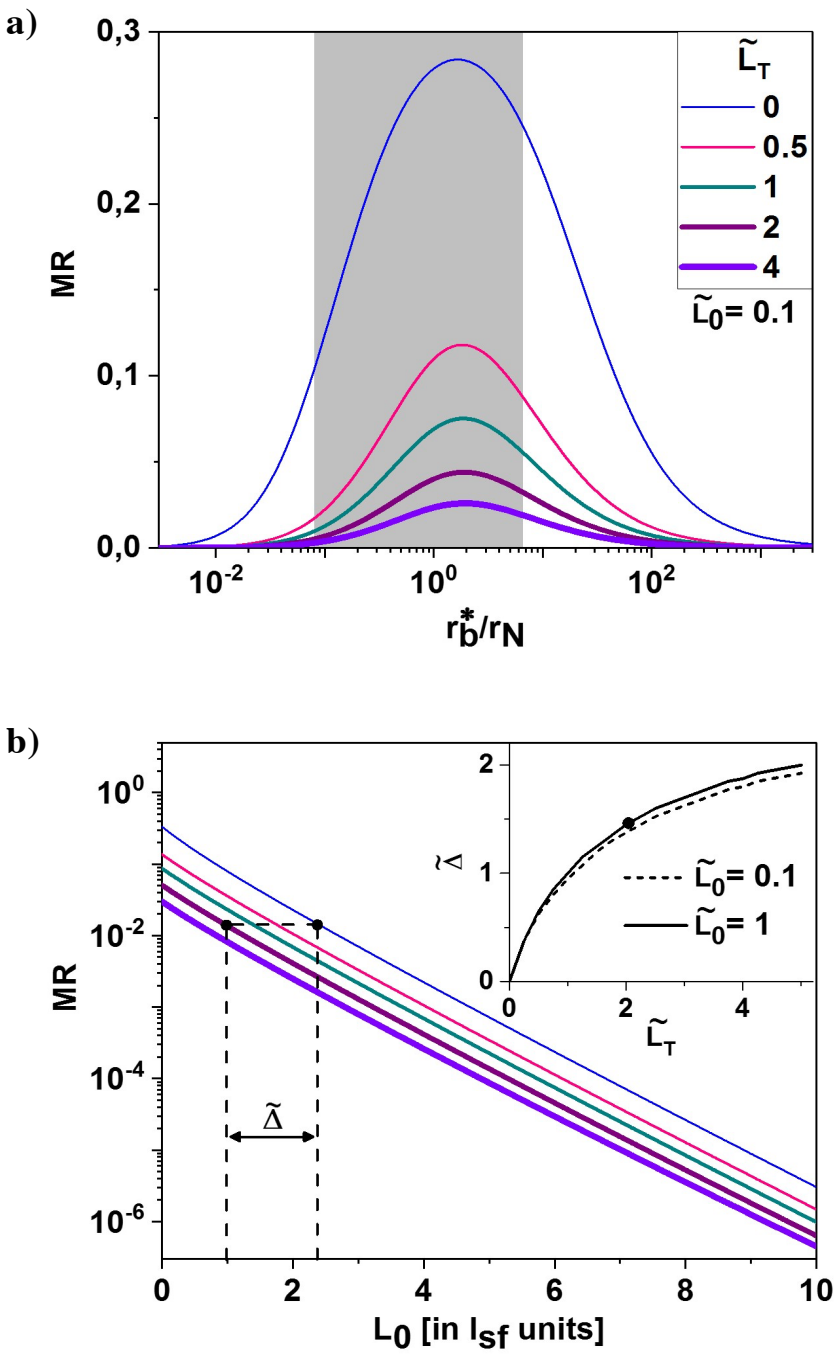

FIG 2. MR ratio calculated from the Fert-Jaffrès model, introducing crowding through Eq. 4. a) variation of the MR with the ratio of interface specific resistance with the spin resistance of the semiconducting spacer. The blue curve is the MR of electrodes separated by 0.1 l_{sf} (without crowding). The other curves illustrate how the MR is reduced when introducing current crowding, of length $\tilde{L}_T$ expressed in l_{sf} units. The shaded area spans the r^*_B/r_N values reported in Table 1; b) MR as a function of electrodes separation, under the hypothesis of optimum r^*_B/r_N value (maximum of the curves in a). The MR follows an exponential variation with electrode separation of slope given by l_{sf} (slope 1 in our scale), with deviations for very short spacing only. For a given MR value (arbitrarily taken at 2%), we indicate the effective increase Δ of channel length that results from crowding (see details in the text), with inset illustrating how Δ increases with the crowding length.

In conclusion, current crowding will significantly diminish MR in planar spin valve devices made of short channel semiconducting layers separating nearby extended electrodes. Calculations predict a significant decrease by up to one order of magnitude, even when taking into account the largest published spin diffusion length values for organics and the shortest crowding lengths reported here. Care should be also taken when interpreting temperature dependent data, as we have seen that the crowding length, and therefore the effective distance between spin current injection and collection points, can vary significantly with temperature. The same can be predicted for gate control of the active channel, as gating will impact the channel as well as the interface resistance values, yet we cannot predict their relative behavior (and therefore the crowding length). Following Eq. (1), it is also essential to measure the material's conductivity and interface resistance values, in order to estimate properly the investigated effective channel length in lateral devices

While our numerical simulations indicate that the spin diffusion length estimates deduced from data obtained with varying the channel lengths should not be affected by crowding corrections, the expected reduction of MR observed in lateral spin valves is of importance for experiments validating organic spin valves. Large spin polarization values of electrodes and interfaces cannot avoid the MR of lateral organic spin valves to hardly exceed the one percent range, which can easily be masked or mimicked by the intrinsic response of the organic semiconductor to a magnetic field, of possible large amplitude.[26] The fringe magnetic field created by the magnetic electrodes can then induces a MR that mimics or blurs a spin valve signal.[27] Data interpretation therefore requires careful analysis of the possibly anisotropic intrinsic magnetic field dependence of the properties of the material used as active channel.[24]

These considerations could be potentially extended to other systems like carbon nanotubes or 2D materials.[28] Even though ballistic charge injection and the significant influence of metallic contacts on 2D materials conductivity make the crowding length possibly different from L_T, an exponential-like current variation approximation remains. Experimental findings on optimum metal-graphene contacts relate to crowding length in the 100 - 400 nm range and values of the order 50-200 nm (thickness-dependent) are reported for MoS_2.[29] For 1D systems, and in particular carbon nanotubes, values as large as 210 μm[30] and as small as 200 nm[31] are found in the literature, reflecting the variability in nanotubes conductivity and contact resistance properties. Even though the expected spin diffusion length is expected to be large for carbon-based nanostructures,[32] current crowding must be taken into account to better estimate spin properties intrinsic to these materials. While these corrections should not affect the outcome of experiments performed using very small contact electrodes experiments on graphene (with expected large l_{sf}), taking into account current crowding effects is mandatory for other 2D semiconductor materials (MoS_2, $MoSe_2$, WS_2) with expected short spin memory lengths and where interfaces play a key role in their transport behavior.[28,33]

ACKNOWLEDGEMENTS

Discussions with M.D. Coey, technical support of STnano cleanroom and F. Chevrier are gratefully acknowledged. Research was partly supported by CNRS Fellowship (T.V.), the Agence Nationale de la Recherche (MULTISELF 11-BS08-06, Labex NIE 11-LABX-0058_NIE within the Investissement d'Avenir program ANR-10-IDEX-0002-02), and the International Center for Frontier Research in Chemistry (icFRC, Strasbourg).

References

[1] D.P. Kenendy, IBM Components Div. Lab. **12**, 242 (1968).
[2] H. Murrmann and D. Widmann, IEEE Trans. Electron Devices **16**, 1022 (1969).
[3] H.S. Ishii K Ito, E Seki, K, Adv. Mater. **11**, + (1999).
[4] D. Natali and M. Caironi, Adv. Mater. **24**, 1357 (2012).
[5] D. Sun, E. Ehrenfreund, and Z. Valy Vardeny, Chem. Commun. **50**, 1781 (2014).
[6] G. Szulczewski, S. Sanvito, and G. Coey, Nat. Mater. **8**, 693 (2009).

[7] X. Zhang, S. Mizukami, T. Kubota, Q. Ma, M. Oogane, H. Naganuma, Y. Ando, and T. Miyazaki, Nat. Commun. **4**, 1392 (2013).
[8] S. Watanabe, K. Ando, K. Kang, S. Mooser, Y. Vaynzof, H. Kurebayashi, E. Saitoh, and H. Sirringhaus, Nat. Phys. **10**, 308 (2014).
[9] T. Kamiya, Y. Kawasugi, M. Ara, and H. Tada, Phys. Rev. B - Condens. Matter Mater. Phys. **95**, 1 (2017).
[10] D. Natali, J. Chen, F. Maddalena, F. Garc??a Ferr??, F. Di Fonzo, and M. Caironi, Adv. Electron. Mater. **2**, 1 (2016).
[11] Y. Xu, C. Liu, W. Scheideler, P. Darmawan, S. Li, F. Balestra, G. Ghibaudo, and K. Tsukagoshi, Org. Electron. Physics, Mater. Appl. **14**, 1797 (2013).
[12] T. Valet and a Fert, Phys. Rev. B **48**, 7099 (1993).
[13] S. Zanettini, G. Chaumy, P. Chávez, N. Leclerc, C. Etrillard, B. Leconte, F. Chevrier, J.-F. Dayen, and B. Doudin, J. Phys. Condens. Matter **27**, 462001 (2015).
[14] M. Galbiati, S. Tatay, S. Delprat, H. Le Khanh, B. Servet, C. Deranlot, S. Collin, P. Seneor, R. Mattana, and F. Petroff, Appl. Phys. Lett. **106**, (2015).
[15] V. Dediu, M. Murgia, F.C. Matacotta, C. Taliani, and S. Barbanera, Solid State Commun. **122**, 181 (2002).
[16] T. Ikegami, I. Kawayama, M. Tonouchi, S. Nakao, Y. Yamashita, and H. Tada, Appl. Phys. Lett. **92**, 153304 (2008).
[17] A. Ozbay, E.R. Nowak, Z.G. Yu, W. Chu, Y. Shi, S. Krishnamurthy, Z. Tang, and N. Newman, Appl. Phys. Lett. **95**, 0 (2009).
[18] W.J.M. Naber, M.F. Craciun, J.H.J. Lemmens, A.H. Arkenbout, T.T.M. Palstra, A.F. Morpurgo, and W.G. van der Wiel, Org. Electron. Physics, Mater. Appl. **11**, 743 (2010).
[19] Y. Kawasugi, M. Ara, H. Ushirokita, T. Kamiya, and H. Tada, Org. Electron. Physics, Mater. Appl. **14**, 1869 (2013).
[20] T.V.A.G. de Oliveira, M. Gobbi, J.M.J.M. Porro, L.E. Hueso, and A.M. Bittner, Nanotechnology **24**, 475201 (2013).
[21] M. Grünewald, J. Kleinlein, F. Syrowatka, F. Würthner, L.W. Molenkamp, and G. Schmidt, Org. Electron. Physics, Mater. Appl. **14**, 2082 (2013).
[22] A. Fert and H. Jaffrès, Phys. Rev. B **64**, 184420 (2001).
[23] T. Verduci, C.S. Yang, L. Bernard, G. Lee, S. Boukari, E. Orgiu, P. Samor??, J.O. Lee, and B. Doudin, Adv. Mater. Interfaces **3**, (2016).
[24] S. Zanettini, J.F. Dayen, C. Etrillard, N. Leclerc, M.V. Kamalakar, and B. Doudin, Appl. Phys. Lett. **106**, 14 (2015).
[25] J.-F. Dayen, V. Faramarzi, M. Pauly, N.T. Kemp, M. Barbero, B.P. Pichon, H. Majjad, S. Begin-Colin, and B. Doudin, Nanotechnology **21**, 335303 (2010).
[26] Y. Wang, K. Sahin-Tiras, N.J. Harmon, M. Wohlgenannt, and M.E. Flatt??, Phys. Rev. X **6**, 1 (2016).
[27] F. Wang, F. Macia, M. Wohlgenannt, A.D. Kent, and M.E. Flatte, Phys. Rev. X **2**, 1 (2012).
[28] A. Allain, J. Kang, K. Banerjee, and A. Kis, Nat. Publ. Gr. **14**, 1195 (2015).
[29] Y. Guo, Y. Han, J. Li, A. Xiang, X. Wei, S. Gao, and Q. Chen, ACS Nano **8**, 7771 (2014).
[30] R. Jackson and S. Graham, Appl. Phys. Lett. **94**, 10 (2009).
[31] A.D. Franklin and Z. Chen, Nat. Nanotechnol. **5**, 858 (2010).
[32] L.E. Hueso, J.M. Pruneda, V. Ferrari, G. Burnell, J.P. Valdés-Herrera, B.D. Simons, P.B. Littlewood, E. Artacho, A. Fert, and N.D. Mathur, Nature **445**, 410 (2007).
[33] D.N. Mouafo, F. Godel, G. Froehlicher, S. Berciaud, B. Doudin, M.V. Kamalakar, and J.-F. Dayen, 2D Mater. **4**, 15037 (2017).